Chinese Journal of Electronics
Vol.32, No.2, Mar. 2023

A Novel Method for Maximum Power Point Tracking of the Grid-Connected Three-Phase Solar Systems Based on the PV Current Prediction

Saeid Bairami[1], Mahdi Salimi[2], and Davar Mirabbasi[1]

(1. *Department of Electrical Engineering, Ardabil Branch, Islamic Azad University, Ardabil, Iran*)

(2. *Faculty of Engineering and Science, University of Greenwich, Medway, Kent, ME4 4TB, UK*)

Abstract — In this paper, it is first attempted to provide a small signal model of the photovoltaic (PV) system, DC-DC boost converter, and pulse width modulation (PWM) generator. Then, a technique is provided for maximum power point tracking (MPPT) in grid-connected solar systems based on variable and adaptive perturbation and observation with predictive control of the PV current. An innovative aspect of the proposed predictive current control method is to use the current controller to achieve the value of PV impedance, which has been used in DC-DC boost converter. The proposed method is to obtain the coming current value on the basis of the current predictive model. The goal of the proposed method is to make the DC-DC boost converter inductor current track the current reference. Voltage and current ripple minimization is added to the cost function simultaneously as a system constraint to optimize system performance. This reduces the amount of voltage and current fluctuations around the maximum power point. The proposed method is capable of detecting rapid changes in solar radiation. A sudden and simultaneous increase in voltage and current is detected by the algorithm and then the duty cycle becomes increasing instead of decreasing. The simulation is carried out in MATLAB Simulink environment in real-time for a 26.6 kW three-phase grid-connected solar system. The simulation results of current predictive control are compared with perturbation and observation techniques and linear voltage and current proportional integral derivative (PID) controller-based adaptive control. The results show that the total harmonic distortion (THD%) of the inverter voltage with proposed method has been reduced by 0.16% compared to the PID method. In addition, the THD% of the current in the proposed method is reduced by 0.1% compared to the PID method. The solar system output voltage variation of the proposed method is less than 5 V.

Key words — Maximum power point (MPP) tracking, Current predictive control, Static converter, Solar system, Power electronics.

I. Introduction

The electricity consumption is expected to become twice by the year 2050 [1]. Despite the development of electrical grids in recent years, the present power systems are not capable of supplying this energy demand sustainably. Hence, it is essential to find clean and renewable energy resources [2]. After a long time, solar systems are a suitable, reliable, and environmentally friendly candidate to supply the electrical energy of consumers [3]. The generating power of solar systems is DC power that is connected to the national grids through DC-DC and DC-AC converters [4]. Given the nonlinear behavior of solar systems in different environmental conditions (ambient radiation and temperature), in order to ensure the proper performance of such energy resources, there is a need for special control algorithms, such as the maximum power point tracking (MPPT) algorithm, and if these algorithms are not used, the system will become unstable [5]. Maximum power point tracking is a process in which the voltage or current of the solar system is adapted to its maximum operating point in different weather conditions [6]. In commercial inverters, maximum power point tracking is done through a DC-DC boost converter. Commercial inverters are usually considered three-phase for powers above 6 kW and single-phase for powers below 6 kW. Different methods have been provided for maxim-

Manuscript Received June 24, 2021; Accepted July 6, 2022.
 DOI:10.23919/cje.2021.00.218

um power point tracking in grid-connected solar systems.

Various techniques are used for MPPT in photovoltaic (PV) systems. There are different methods, including perturbation and observation (P&O) algorithm [7], incremental conductivity (INC) [8], constant voltage (CV) [9], open voltage (OC) method [10], voltage or current feedback method [11], closed-loop voltage control, PID controller-based PV current [12], fuzzy logic control [13], adaptive neural network for tracking. Unfortunately, two critical problems can be seen in conventional methods, one problem is the impossibility of creating an interaction between the dynamic behavior of MPPT algorithm and fluctuations around the maximum power point in the steady state of the system. Another problem is the need for high computational volume to reach the optimal point of the work. Among other problems with such methods is the low-speed response of the system during sudden changes in solar radiation.

One of the most popular tracking methods is the P&O algorithm, however, this method has certain disadvantages. The incidence of a large disturbance on the side of the solar system will cause severe fluctuations on the side of the grid [10]. In addition, the lack of quick response and fluctuations around the operating point is the other disadvantages of this algorithm. The incremental conductivity algorithm is another well-known for MPPT. The lack of access to the exact operating point and hardware problems for implementation are the major disadvantages of this method [11]. To improve the performance of the above methods, an improved P&O technique is proposed based on proportional integral derivative (PID), which has better stability than the previous methods. However, this method depends on PID controller parameters, which are very complex to regulate [12]. In recent years, intelligent algorithms have been used in maximum power point tracking. The fuzzy logic-based improvement method is one of these techniques [13]. The performance of fuzzy logic control and neural network control is very dynamic and stable in maximum power point tracking. However, the design of this controller requires a lot of skill and experience, and the long calculation time and the need for digital signal processing are the disadvantages of these techniques. One of the improved methods in maximum power point tracking is to use compulsory learning algorithms. In recent years, digital control methods for maximum power point tracking in distributed and renewable energy resources have grown dramatically. The current predictive control method and powerful current predictive control technique are two examples of these methods. Among the various tracking methods, the current predictive control method is more popular. Limited switching, low cost, fast response, and high dynamics are the advantages of this control method.

In this paper, it was first attempted to provide a small signal model of the PV system, DC-DC boost converter, and pulse width modulation (PWM) generator. Then, a technique is provided for MPPT in grid-connected solar systems based on variable and adaptive perturbation and observation with PV current predictive control. An innovative aspect of the proposed current predictive control method is to use the current predictive control to achieve the value of PV inductance based on the PV current predictive model, which has been used in the DC-DC boost converter. The proposed method is to obtain the coming current value on the basis of the current predictive model. The cost function consists of at least one controlled variable reference tracking section, which can be current, voltage, torque, and so on. The goal of the proposed method is to minimize the voltage and current ripple to optimize the system performance by adding to the cost function simultaneously as a system constraint. Accordingly, an additional part in the cost function is considered as the difference between the measured value of voltage in the current and the next state. In order to optimize the voltage ripple, a meta-heuristic mehod, namely arithmetic optimization algorithm (AOA) has been used [14].

II. Main Components of the Solar System Modeling

In Fig.1, the integration of a solar system with a distribution grid is shown through a two-stage static converter. A grid integration system includes solar arrays, DC-DC boost converter, DC-AC inverter, and LCL filter. The generating power of solar arrays is DC, which is a function of solar function and ambient temperature [8]. A mathematical model is often used for modeling short-term solar systems. In practice, solar systems can be modeled as a variable voltage resource or variable current resource [9]. For a proper understanding of the effects of radiation and temperature on the generating power of the solar system, a current resource model is used for simulation.

The main notations used in this paper are listed below:

I_{D} — Diode current (A);
I_{O} — Diode saturation current (A);
V_{C} — Cell voltage (V);
q — Electron charge (1.6×10^{-19} C);
A — Ideal diode constant;
K — Boltzmann's constant(1.38×10^{-23} J/K);
T_{C} — Cell temperature (K);
N_{S} — Number of modules in series in the solar ar-

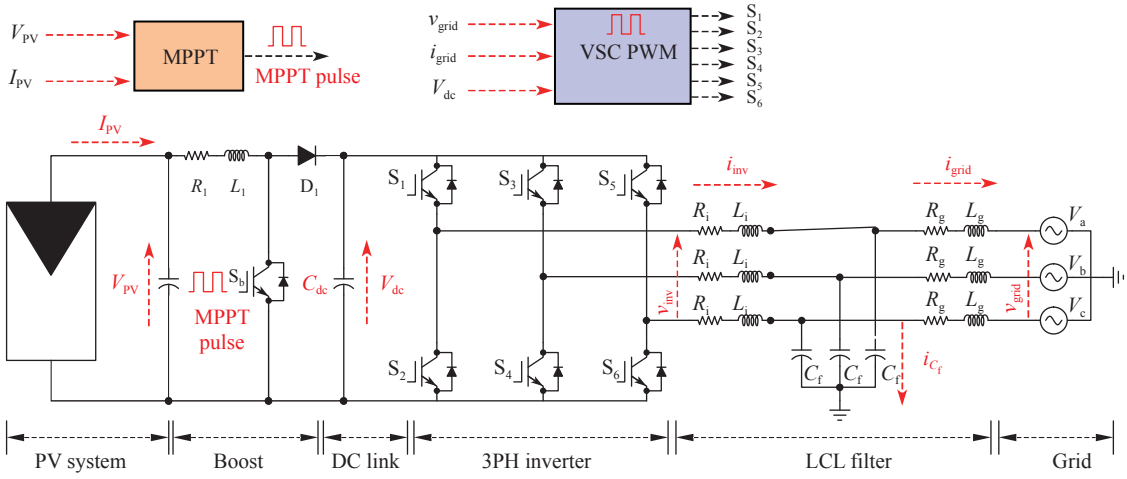

Fig. 1. Grid-connected solar system with a two-stage static converter.

ray;

N_P — Number of parallel modules in the solar array;

n_S — Number of cells in the solar module;

I_{SC} — Current generated by solar radiation in the module;

R_{se} — Series resistance of module;

R_{sh} — Parallel resistance of module;

V_D — Diode double voltage;

V_g — Energy vacuum band (eV);

I_{rs} — Reverse saturation current.

An ideal solar cell can be theoretically simulated by a current resource in series with a diode. In Fig.2, an improved model of a solar cell is shown in which the effects of series and parallel resistance have been observed.

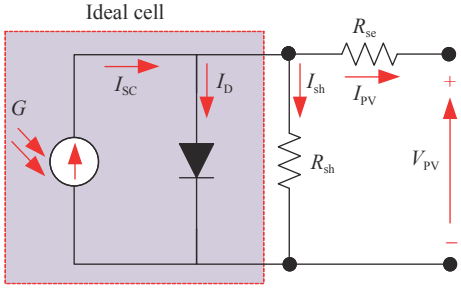

Fig. 2. An ideal solar cell with series and parallel resistances.

According to the Shockley equation, the current is as follows [3]:

$$I_D = I_O \times \left(e^{\frac{V_C q}{AKT_C}} - 1\right) \tag{1}$$

In general, the cell current is obtained from the current difference between the current generated by solar radiation and the diode current [4]:

$$I_{PV} = I_{SC} - I_D \tag{2}$$

In the real operation of solar cells, there are some losses that must be added to the model. In practice, these losses are added as a series resistance and parallel resistance to the model to make the operation of the simulated system more realistic. To show the V-I curve in the solar system, there is a need for adding other additional parameters [2].

$$I_{PV} = N_P I_{SC} - N_S I_O \times \left(e^{\frac{(V+IR_{se})q}{n_S AKT_C}} - 1\right) - \frac{V + \frac{N_S}{N_P} IR_{se}}{R_{sh}} \tag{3}$$

It is shown in (3) that the output current of generation depends on the module voltage, solar radiation, and ambient temperature. The characteristic equation V-I of the circuit of Fig.2 will be as follows [3]:

$$I_{PV} = I_{SC} - I_D - \frac{V_D}{R_{sh}} \tag{4}$$

Saturation current of the cell diode is as follows:

$$I_O = I_{rs}\left[\left(\frac{T}{T_{ref}}\right)^3 e^{\frac{qV_g}{AK\left(\frac{1}{T_{ref}} - \frac{1}{T}\right)}}\right] \tag{5}$$

This equation shows that the diode saturation current depends on the cell temperature. The inverse saturation current is obtained from the following equation [4]:

$$I_{rs} = I_{SCref}\left[e^{\frac{qV_{OC}}{N_S KAT}} - 1\right] \tag{6}$$

In the end, the output power of the solar system is as follows [5]:

$$P_{PV} = V_{PV} \times \left[N_P I_{SC} - N_S I_O \times \left(e^{\frac{(V+\frac{N_S}{N_P} IR_{se})q}{n_S AKT_C}} - 1\right) - \frac{V + IR_{se}}{R_{sh}}\right] \tag{7}$$

III. Small Signal Model of Solar System

The current resource model of a solar cell is already shown in Fig.2. In the current resource model, the equivalent resistance value of the solar panel is as follows:

$$\begin{aligned} R_{\rm eq} &= R_{\rm se} + R_{\rm sh} \\ R_{\rm se} &= \frac{V_{\rm OC} - V_{\rm MPPT}}{I_{\rm MPPT}} \\ R_{\rm sh} &= \frac{V_{\rm MPPT}}{I_{\rm SC} - I_{\rm MPPT}} - R_{\rm se} \end{aligned} \tag{8}$$

Pulse generation in pulse width modulation is done through the comparison of carrier signal with the input signal $V_{\rm ref}$. The resulting output signal is applied to the DC-DC converter as the switching cycle. The conversion function of pulse width modulation is a linear equation compared to the switching cycle signal (D) and is defined as follows [6]:

$$\frac{D(s)}{V_{\rm com}} = \frac{1}{V_{\rm P}} \tag{9}$$

In conventional pulse width modulation, the value of $V_{\rm P} = 1$ is considered.

The transfer function of voltage control and input current compared to the switching cycle (D) of the incremental converter, considering the effects of equivalent resistance $R_{\rm eq}$ and $C_{\rm dc}$, will be defined as follows:

$$\begin{aligned} G_{V/D}(s) &= \frac{V_{\rm PV}}{D(s)} = \frac{C_{\rm dc}R_{\rm eq}V_{\rm dc}s + D'I_{\rm PV}R_{\rm eq}}{C_{\rm dc}C_{\rm PV}LR_{\rm eq}s^3 + C_{\rm dc}Ls^2 + (C_{\rm PV}R_{\rm eq}D'^2 + C_{\rm dc}R_{\rm eq})s + D'^2} \\ G_{I/D}(s) &= \frac{I_{\rm PV}}{D(s)} = \frac{C_{\rm dc}C_{\rm PV}R_{\rm eq}V_{\rm dc}s^2 + (C_{\rm dc}V_{\rm dc} + C_{\rm PV}D'I_{\rm PV}R_{\rm eq})s + D'I_{\rm PV}}{C_{\rm dc}C_{\rm PV}LR_{\rm eq}s^3 + C_{\rm dc}Ls^2 + (C_{\rm PV}R_{\rm eq}D'^2 + C_{\rm dc}R_{\rm eq})s + D'^2} \end{aligned} \tag{10}$$

where $D' = 1 - D$.

IV. Maximum Power Point Tracking (MPPT)

1. Closed-loop control of voltage and current with PID

One of the oldest methods for maximum power point tracking in solar systems is to use the closed loop voltage and current control based on the linear PID controller. This maximum power point tracking includes two parts, a closed-loop voltage system, and a closed-loop current regulator. Fig.3 shows the block diagram of the closed-loop voltage and current based on the PID control.

As shown in Fig.3, the error resulting from comparing the solar system voltage with the reference voltage is applied to a PID controller. The output of the PID controller of voltage is defined as the reference current $I^*_{\rm PV}$. The main current of the solar system is compared with current $I^*_{\rm PV}$ and is applied to another PID controller. The output signal from the PID is applied to the DC-DC converter as the switching cycle signal (D) [2].

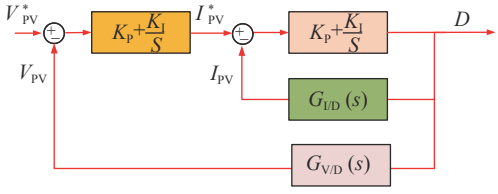

Fig. 3. Block diagram of the closed loop voltage and current based on PID control.

Block diagram of closed loop voltage and PV current with PID control of a grid-connected solar system is shown in Fig.4. PID parameters are regulated using (10) and SISO-Tool features of MATLAB software. Table 1 indicates the PID parameters obtained for a 26.6 kW solar system with the specifications of Table 2 and Bode plot, Nyquist plot, root locus, and step response of the compensated function $G_{CV} \times G_{V/D}(s)$ (see Fig.5) and $G_{CI} \times G_{I/D}(s)$(see Fig.6).

As shown in Fig.5, the step response of the compensated system in the voltage control loop had a fast response and the poles were on the negative side and

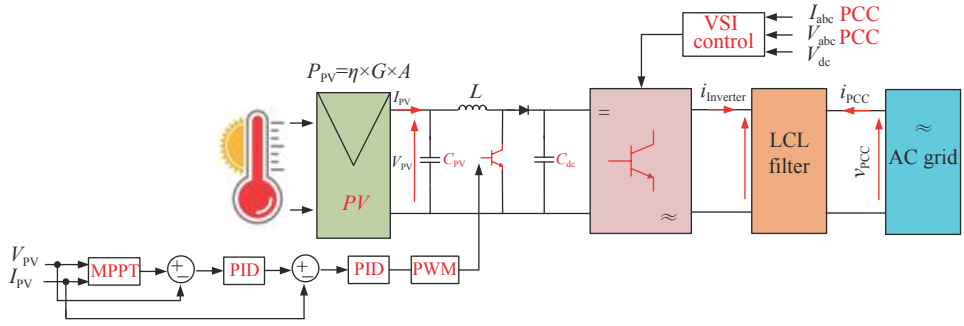

Fig. 4. Block diagram of the distribution grid-connected solar system with maximum power point tracking of closed loop voltage and current based on the linear PID controller.

Table 1. PID controller parameters for maximum power point tracking

	P	I	D
$G_{V/D}(s)$	2	1.5	5.751E−5
$G_{I/D}(s)$	0.254	0.305	5.751E−3

stabilize the system.

Additionally, in Fig.6, the step response of the current control loop is shown, as can be seen, the function response is slow but lacks any overshot.

Table 2. 26.6 kW solar system parameters

Parameter	Value
C_{PV}	60 μF
L	85 μH
f_{sw}	5 kHz
C_{dc}	6.8 mF
DC link voltage	500 V
$V_{\max}$	243 V
Power PV	26.6 kW

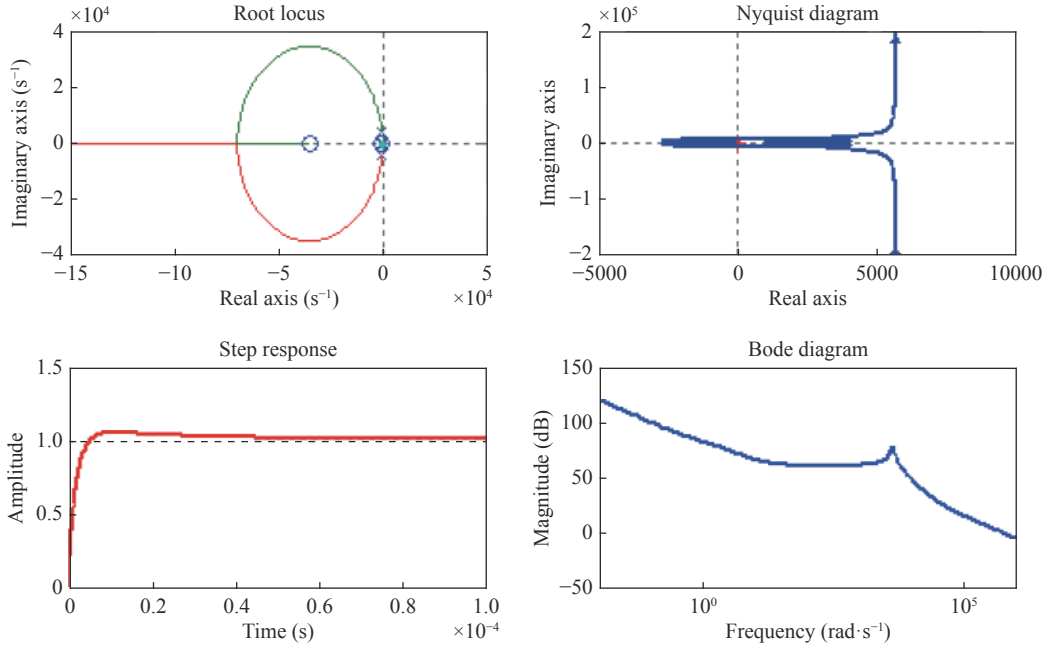

Fig. 5. Root locus, Nyquist diagram, step response, and Bode plot of compensation function $G_{CV} \times G_{V/D}(s)$.

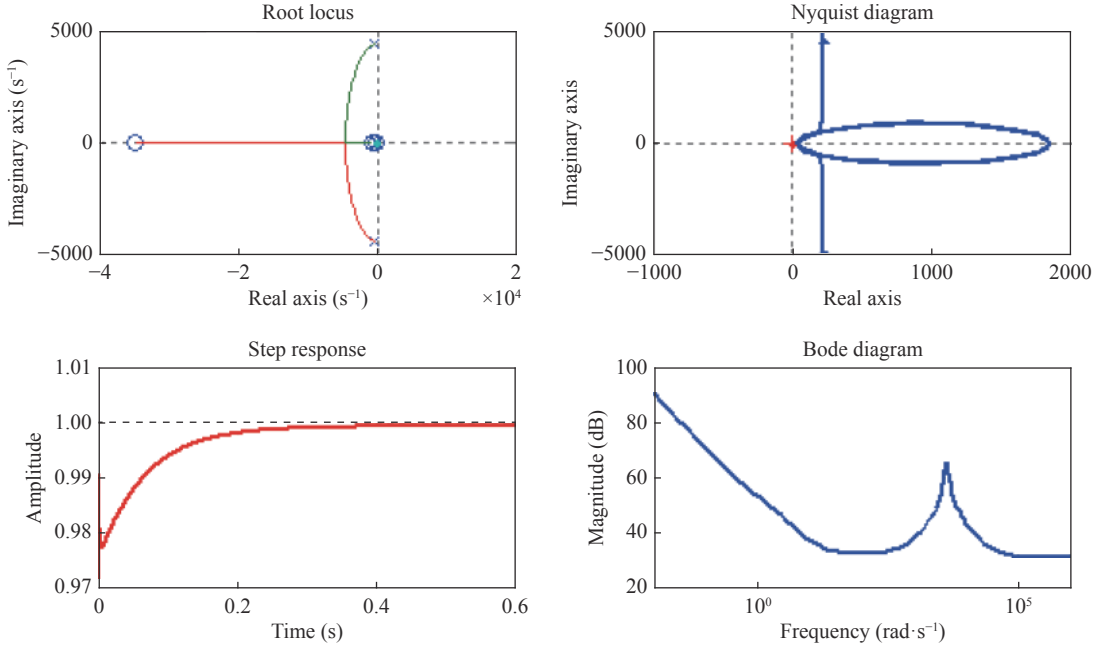

Fig. 6. Root locus, Nyquist diagram, step response, and Bode plot of compensation function $G_{CI} \times G_{I/D}(s)$.

2. Proposed method

PV current predictive control method is a technique to determine the value of leading current based on present current of the system (see Fig.7). When the incremental converter switch is ON, the PV current is calculated as follows [12]:

$$L\frac{dI_{\rm PV}}{dt} = V_{\rm PV} \tag{11}$$

When the incremental converter switch is OFF, the PV current is calculated as follows:

$$L\frac{dI_{\rm PV}}{dt} = V_{\rm PV} - V_{\rm dc} \tag{12}$$

For a sampling period ($T_{\rm s}$), the derivative form $\frac{dI_{\rm PV}}{dt}$ is redefined as follows:

$$L\frac{dI_{\rm PV}}{dt} = L\frac{I_{\rm PV}(k+1) - I_{\rm PV}(k)}{T_{\rm s}} \tag{13}$$

In both ON and OFF modes of DC-DC converter, the current predictive current is defined as follows [10]:

$$I_{\rm P}(k+1) = I_{\rm PV}(k) + \frac{T_{\rm s}}{L}V_{\rm PV}(k) \tag{14}$$

$$I_{\rm P}(k+1) = I_{\rm PV}(k) + \frac{T_{\rm s}}{L}(V_{\rm PV}(k) - V_{\rm dc}(k)) \tag{15}$$

The main purpose of current predictive current control is inductance current tracking of converter from the reference current. Assuming the present switching cycle ($D(k)$) and that the PV current is equal to the inductance current of the converter, formula (15) can be redefined as follows:

$$\begin{aligned} I_{\rm P}(k+1) =& I_{\rm PV}(k) + \frac{D(k)T_{\rm s}}{L}V_{\rm PV}(k) \\ &+ \frac{T_{\rm s}(1-D(k))}{L}(V_{\rm PV}(k) - V_{\rm dc}(k)) \end{aligned} \tag{16}$$

Therefore, the switching cycle ($D(k)$) will be as follows:

$$D(k) = 1 - \frac{1}{V_{\rm dc}(k)}\left[\frac{L}{T_{\rm s}}(I_{\rm PV}(k) - I^*_{\rm PV}(k+1) + V_{\rm PV}(k))\right] \tag{17}$$

where, $I^*_{\rm PV}(k+1)$ will be calculated as follows:

$$I^*_{\rm PV}(k+1) = 3(I^*_{\rm PV}(k) - I^*_{\rm PV}(k-1) + I^*_{\rm PV}(k-2)) \tag{18}$$

The basis of the proposed method of current predictive current is as follows:

- The voltage, current and power of system in the kth period is measured using a sensor.
- In a sampling period (20 ms), two subsequent samples of power at the present moment are compared with previous moments.
- Power variations (ΔP) are calculated and then the reference voltage is decreased and increased in proportion to this value.

Eventually, the reference voltage is calculated using the parameters in the current predictive control method.

The cost function is the main difference between MPC and other predictive control strategies. Basically, this is a collective function that includes various subfunctions that represent our demands on the control system. The cost function consists of at least one controlled variable reference tracking section, which can be current, voltage, torque, and so on. In this paper, voltage and current ripple minimization is added to the cost function simultaneously as a system constraint to optimize system performance. Accordingly, an additional part in the cost function is considered as the difference between the measured value of voltage in the current and next state. In order to optimize the voltage ripple, the arithmetic optimization algorithm has been used [14].

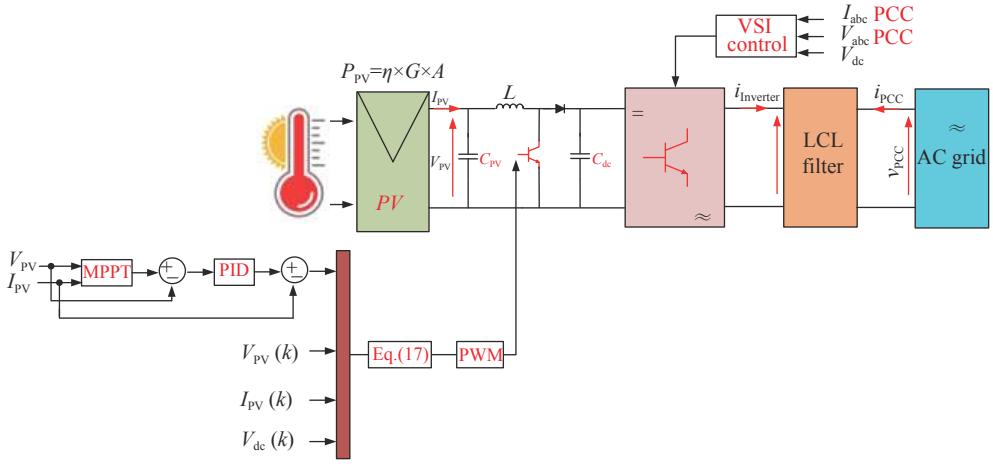

Fig. 7. Block diagram of a solar system connected to the distribution grid with maximum power point tracking of PV current predictive.

V. Simulation Results

In this study, BP Solar SX3190 solar panels are used and the technical specifications are listed in Tables 3–5. The voltage-power and voltage-current curves are shown in Figs.8 and 9 per composition (10 cells in series and 14 cells in parallel), also I_{SC} and I_{sat}, V_m and R_m are shown in Figs.10 and 11.

Table 3. BP Solar SX3190 module specifications

Parameter	Variable	Value
Maximum power	P_m	190 W
Maximum voltage	V_m	24.3 V
Maximum current	I_m	7.85 A
O.C Voltage	V_{OC}	30.6 V
S.C Current	I_{SC}	8.5 A
Cells in series	N_S	50

Table 4. Maximum current and voltage in the BP Solar SX3190 module

$G(W/m^2)$	1000	750	500	250	100
$V_m(V)$	243	242.8	240.7	233.7	220.3
$I_m(A)$	109.6	81.9	54.2	26.3	10.14
$R_m(\Omega)$	2.217	2.964	4.443	8.873	20.792

Table 5. Series and parallel resistance, modulus diode saturation current

$T(°C)$	0	25	50	75	100
$I_O(A)$	1E−9	4E−8	9E−5	1E−5	1E−4
$R_{sh}(\Omega)$	479	189	120	107	267
$R_{se}(\Omega)$	0.249	0.248	0.254	0.277	0.316

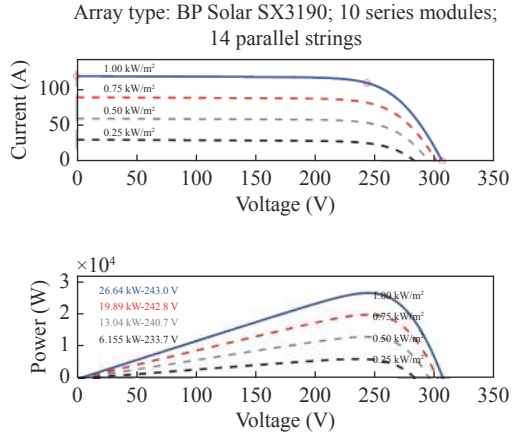

Fig. 8. V-I and V-P curve in BP Solar SX3190 module.

A 26.6 kW solar system was simulated in MATLAB Simulink environment and in real-time. The running time of the simulation is 2.5 s. According to Fig.12, the solar radiation is reduced from 1000 W/m^2 to 100 W/m^2 in this period. The simulation results include changes in voltage and current of the solar system, DC link, PV power generation changes, maximum power point tracking, and study of power quality parameters

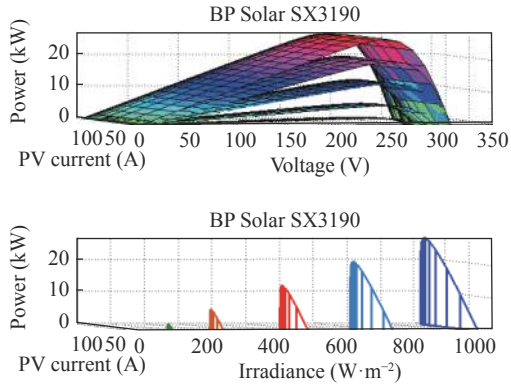

Fig. 9. (3-D) V-I and V-P curve in BP Solar SX3190 module.

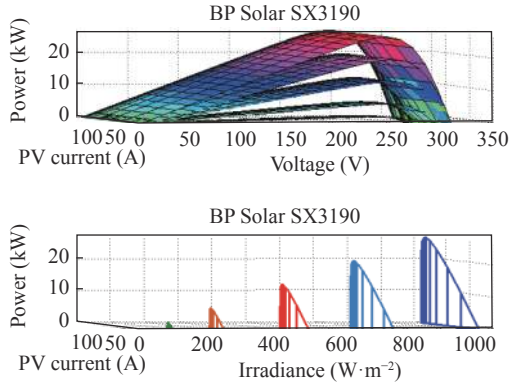

Fig. 10. (3-D) I_{SC} and I_{sat} current in BP Solar SX3190 module.

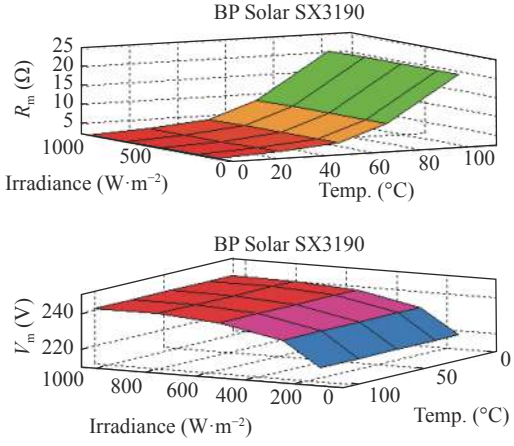

Fig. 11. (3-D) R_m and V_m in BP Solar SX3190 module.

on the inverter output.

In Figs.13–18, it has been shown that tracking in current predictive current control is much more accurate than other existing methods. The amount of fluctuations around the operating point in the proposed method is less than other methods. According to Figs.17 and 18, the fluctuations of system power generation and DC link voltage with current predictive current controller have a better performance than PID and P&O. The ripple power of the proposed method is about 0.02 kW (see Table 6). In Fig.19, it is shown that the maximum

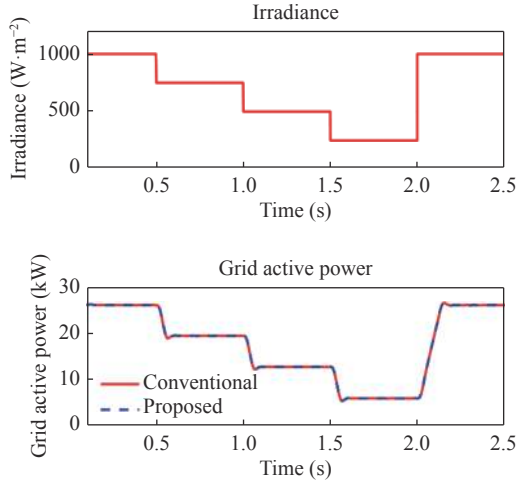

Fig. 12. Solar radiation changes during the simulation period.

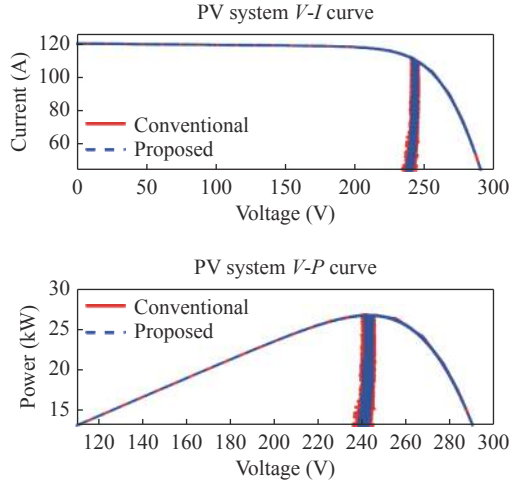

Fig. 13. Fluctuations around the operating point with the proposed and PID methods.

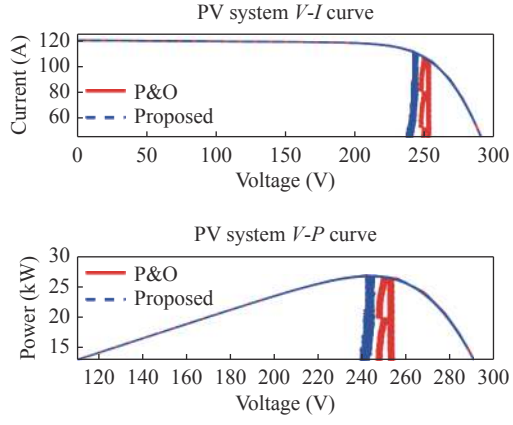

Fig. 14. Fluctuations around the operating point with the proposed and P&O methods.

resistance value (R_{MPPT}) with the proposed method is much closer to the reference value.

As shown in Figs.20–23, the total harmonic distortion (THD%) of the inverter voltage with proposed

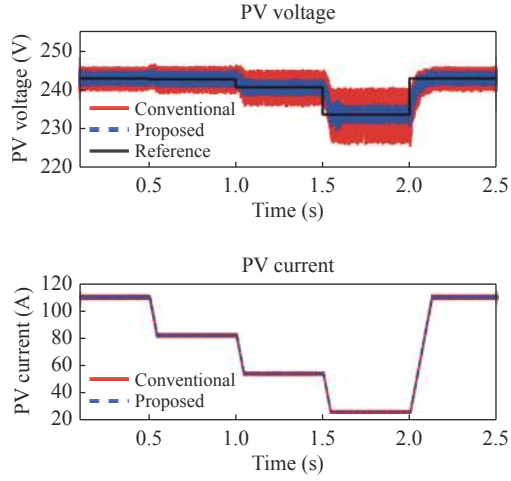

Fig. 15. PV voltage and current with the proposed and PID methods.

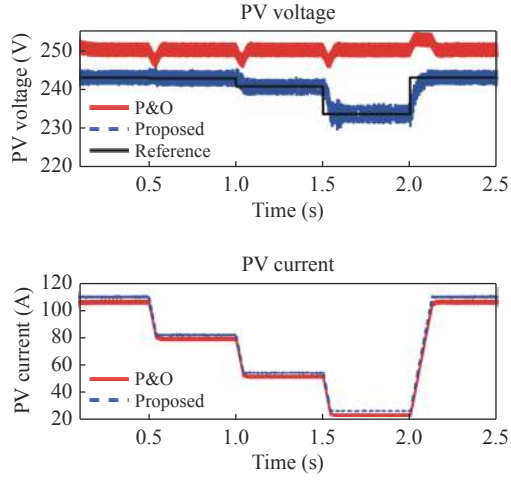

Fig. 16. PV voltage and current with the proposed and P&O methods.

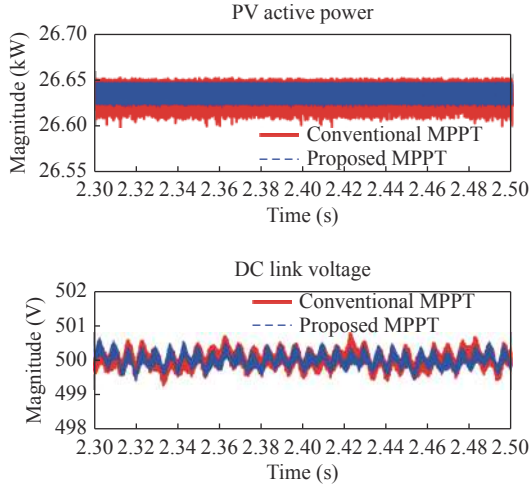

Fig. 17. PV power and DC link voltage with PID and proposed method.

method has been reduced by 0.16% compared to the PID method. In addition, the THD% of the current in

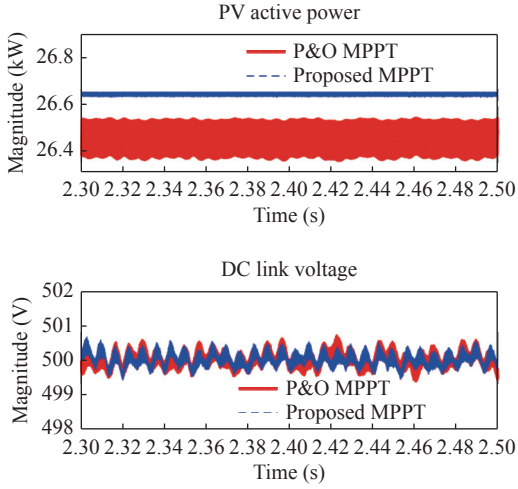

Fig. 18. PV power and DC link voltage with P&O and proposed method.

Table 6. Comparing the results of different methods

Method	Ripple power (W)	Ripple current (A)	Ripple voltage (V)
Proposed method	20	5	5
PID	100	13	8
P&O	60	20	15

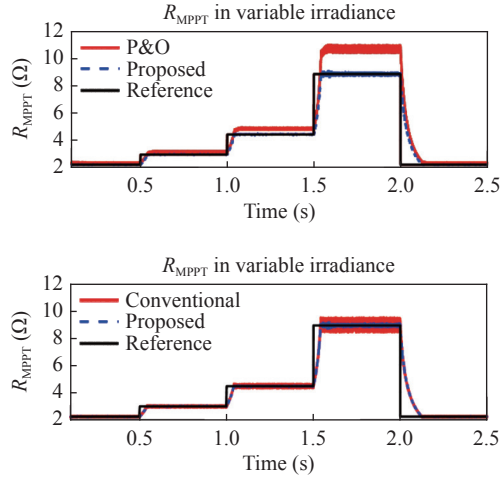

Fig. 19. Comparison of maximum resistance R_{MPPT} in different method.

the proposed method is reduced by 0.1% compared to the PID method.

VI. Experimental System and Results

1. Experimental system

The boost converter circuit comprises a DC voltage source, an inductor, and an electronic switch, with MOSFET components, diodes, capacitors, and resistors serving as loads. On this circuit, an IRF250 MOSFET with sufficient V_{gs} over a 600-V voltage range was used, and also had small enough R_{ds} to increase the load capacity of this circuit (Fig.24).

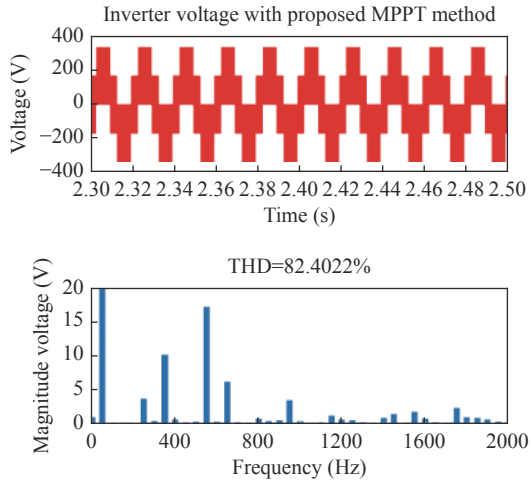

Fig. 20. Inverter output voltage quality with the proposed method.

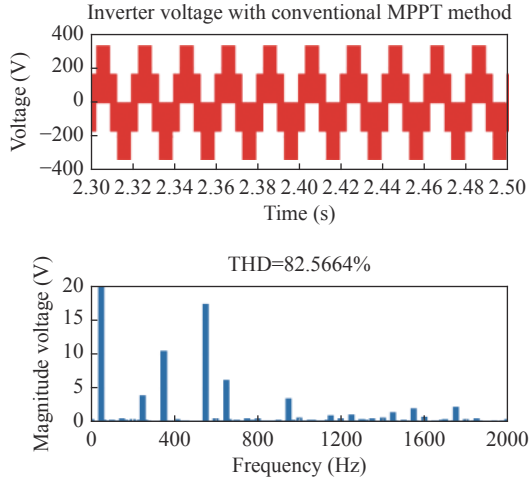

Fig. 21. Inverter output voltage quality with PID method.

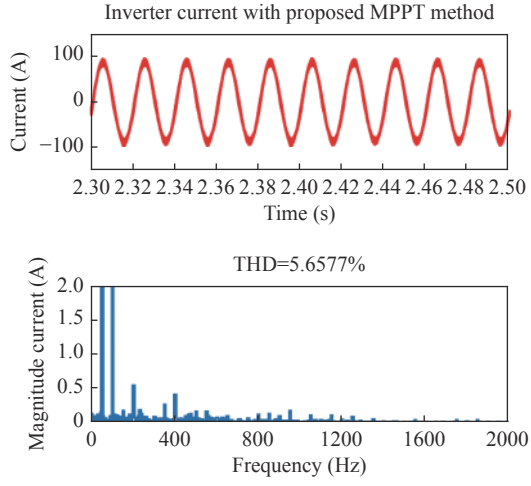

Fig. 22. Inverter output current quality with the proposed method.

The ACS712 is a current sensor that operates on the principle of field effects. This current sensor is capable of measuring both AC and DC. This sensor mod-

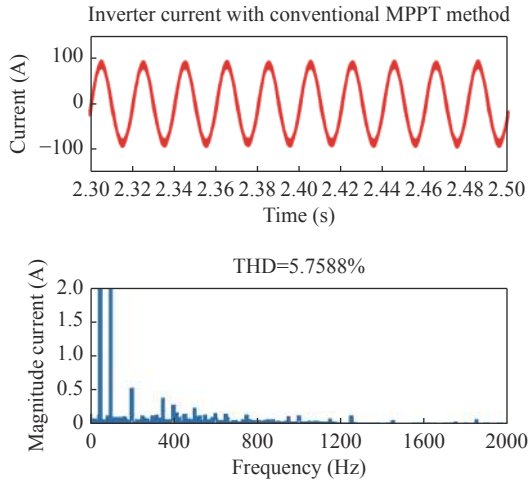

Fig. 23. Inverter output current quality with PID method.

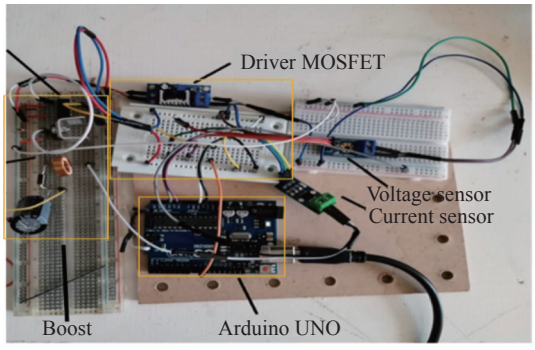

Fig. 24. Design and experimentation of a boost converter.

ule includes an operational amplifier circuit, which increases the sensitivity of the current measurement and enables it to detect minimal current changes.

The voltage sensor used in this paper was the Arduino voltage sensor, which allowed for the reading of a circuit's voltage value. Analog pins on the Arduino enable it to read voltage values.

The IR2110/IR2113 are high-voltage, high-speed power MOSFET and IGBT drivers with independently referenced output channels on the high and low sides.

Arduino Uno R3 is a minimum system board based on the AVR microcontroller type ATmega328P. The BP SX3190 solar panels which used in the experiment is shown in Fig.25.

Fig. 25. BP SX3190 solar panels which used in the experiment.

2. Experimental results

To evaluate the performance of the PV system, an experiment has been carried out. Here, the results of the experiment are represented. The set of experimental results are shown in Fig.26. This experiment shows the inverter response to rappidly variations of the radiation. In this experiment, the radiation changes rappidly between 1000 to 100 with step of 250 per 1.75 s intervals. The frequency of the inverter is 5 kHz. It can be properly concluded that the inverter follows these rappidly changes of the radiation which can be seen in the waveforms of the output voltage and current.

One of the challenges faced by the MPPT algorithms is on reaching the global MPP under partial shading condition. Another experiment have been done under partial shading conditions. The results of this important experiment are presented in Fig.27 and Fig.28.

Comparison of practical and simulation results shows that the production capacity is consistent and the proposed method can have high accuracy of tracking in partial shading conditions.

One important set of methods, called software-based GMPP tracking (GMPPT) algorithms, identifies the GMPP of a multiple peak P-V curve of a PV array without hardware modifications, since it can be included as routines in the inverter controller. A reliable GMPPT algorithm must correctly find the GMPP for a P-V curve with any number of peaks. On the other hand, reliable GMPPT algorithms that track the GMPP under any PSC have been proposed in [15]. However, to obtain reduced energy losses, GMPPT algorithms must also be as fast as possible.

Model predictive current control method has a faster dynamic and better steady-state response. But, the dynamic and steady-state response depends on step size in the production of the reference current in MPC method. In the proposed method under uniform conditions, the PI controller applied to the error between the initial reference current from P&O and the actual current of the photovoltaic array. The reference current from the PI controller and the predictive current are applied to the cost function and the required switching pulses are generated.

The simulation and experimental results show that the proposed method has a faster dynamic response and low steady-state power ripple. The simulation and experimental results demonstrates that the MMPC method tracks the MPP more accurately and quickly than the MPC method under PSC[16,17].

VII. Conclusions

In this paper, the maximum power point tracking in a solar system connected to the distribution grid was

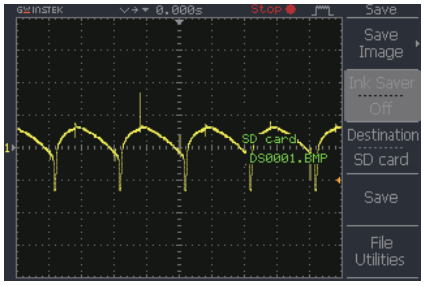

(a)

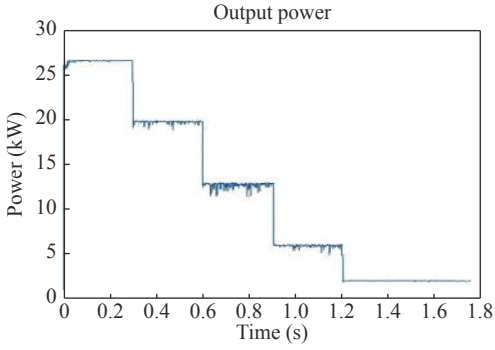

(b)

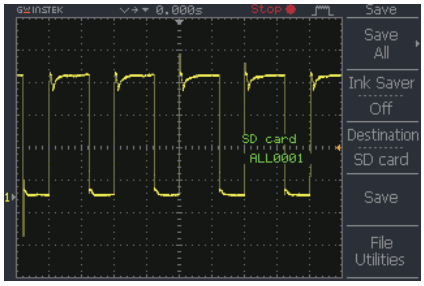

(c)

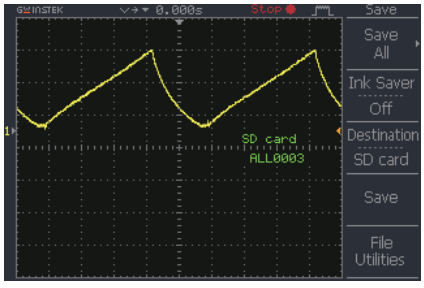

(d)

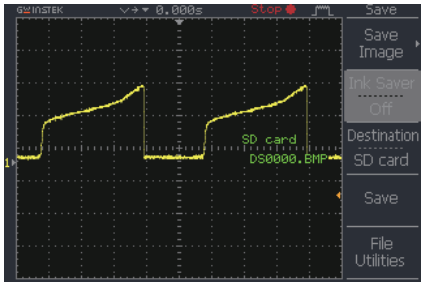

(e)

Fig. 26. The results of the experiment. (a) Output voltage; (b) Output power; (c) Duty cycle; (d) Inductor current; (e) MOSFET I_D current.

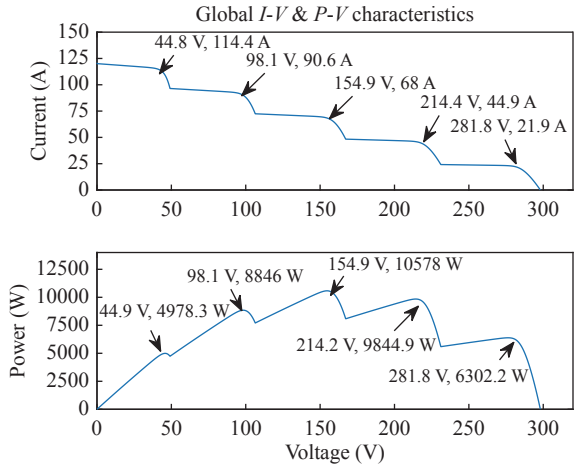

Fig. 27. Curves of a 10-module PV array with each module under different random irradiances ≤ 1000 W/m^2 at $T = 25$ °C.

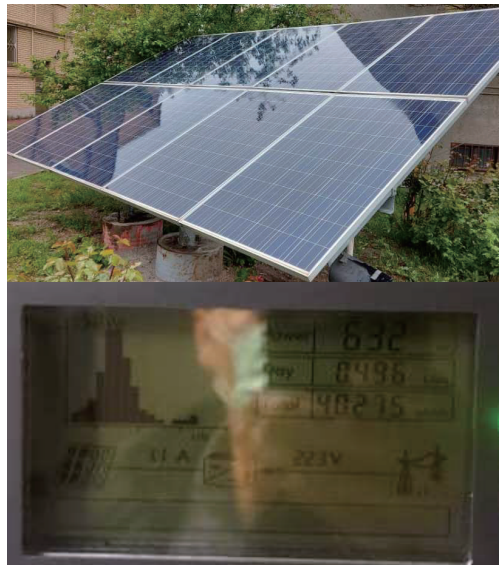

Fig. 28. picture panel and inverter experimental in partial shading.

analyzed using three methods of P&O, closed loop voltage and current control with PID controller, and maximum power point tracking with PV current predictive current. The simulation is performed in Matlab/Simulink environment and in real-time for a 26.6 kW three-phase grid-connected solar system. The simulation results are compared with current predictive control, P&O techniques, closed-loop voltage control, and PID controller-based PV current. The results show that the proposed control method has the lowest fluctuations around the operating point. The proposed method has also improved power quality parameters. The results showed that voltage, current, and output power at the MPP point with PV current predictive control has a much better performance. The AOA optimization algorithm was applied to minimize the voltage and

current ripple. Therefore, in the proposed maximum power point tracking algorithm, a decrease can be seen in voltage and current fluctuations around the operating point. Additionally, it was shown that the proposed method has a better response rate than the changes in the radiation. Based on the experimental results, the output power of the system in the proposed method has also a better performance than other methods. It is also shown that the lower the fluctuations around the operation, the quality of the voltage and current delivered to the inverter will be improved.

Acknowledgements: This paper is the outcome of Ph.D. thesis of Mr. Saeid Bairami at the Islamic Azad University – Ardabil Branch.

References

[1] Z. Song, Y. Tian, W. Chen, Z. Zou, and Z. Chen, "Predictive duty cycle control of three-phase active-front-end rectifiers," *IEEE Transactions on Power Electronics*, vol.31, pp.698–710, 2015.

[2] S. Motahhir, A. El Hammoumi, and A. El Ghzizal, "Photovoltaic system with quantitative comparative between an improved MPPT and existing INC and P&O methods under fast varying of solar irradiation," *Energy Reports*, vol.4, pp.341–350, 2018.

[3] S. Sajadian and R. Ahmadi, "Model predictive-based maximum power point tracking for grid-tied photovoltaic applications using a Z-source inverter," *IEEE Transactions on Power Electronics*, vol.31, pp.7611–7620, 2016.

[4] H. Rezk, A.-O. Mazen, M. R. Gomaa, M. A. Tolba, A. Fathy, M. A. Abdelkareem, " A novel statistical performance evaluation of most modern optimization-based global MPPT techniques for partially shaded PV system," *Renewable and Sustainable Energy Reviews*, vol.115, article no.109372, 2019.

[5] K. Sundareswaran, V. Vigneshkumar, P. Sankar, S. P. Simon, P. S. R. Nayak, and S. Palani, " Development of an improved P&O algorithm assisted through a colony of foraging ants for MPPT in PV system," *IEEE Transactions on Industrial Informatics*, vol.12, pp.187–200, 2015.

[6] J.-C. Kim, J.-H. Huh, and J.-S. Ko, " Improvement of MPPT control performance using fuzzy control and VGPI in the PV system for micro grid," *Sustainability*, vol.11, article no.5891, 2019.

[7] K.-Y. Chou, S.-T. Yang, and Y.-P. Chen, "Maximum power point tracking of photovoltaic system based on reinforcement learning," *Sensors*, vol.19, article no.5054, 2019.

[8] M. H. Anowar and P. Roy, " A modified incremental conductance based photovoltaic MPPT charge controller," *2019 International Conference on Electrical, Computer and Communication Engineering (ECCE)*, Cox's Bazar, Bangladesh, pp.1–5, 2019,.

[9] K. Ali, L. Khan, Q. Khan, S. Ullah, S. Ahmad, S. Mumtaz, *et al.*, "Robust integral backstepping based nonlinear MPPT control for a PV system," *Energies*, vol.12, article no.3180, 2019.

[10] J. Gosumbonggot and G. Fujita, " Global maximum power point tracking under shading condition and hotspot detection algorithms for photovoltaic systems," *Energies*, vol.12, article no.882, 2019.

[11] W. Xu, C. Mu, and L. Tang, "Advanced control techniques for PV maximum power point tracking," in *Advances in Solar Photovoltaic Power Plants*, Springer, pp.43–78, 2016.

[12] A. Kusuma, M. Hakim, G. Alvianingsih, D. Aryani, and A. Utomo, "An improved P&O algorithm for single-stage grid-connected photovoltaic system under rapidly changing environment conditions," *International Conference on Green Energy and Environment*, Pangkal Pinang, Indonesia, article no. 012016, 2019.

[13] C. C. Hua, Y. H. Fang, and C. J. Wong, "Improved solar system with maximum power point tracking," *IET Renewable Power Generation*, vol.12, pp.806–814, 2018.

[14] L. Abualigah, A. Diabat, S. Mirjalili, M. Abd Elaziz, and A. H. Gandomi, " The arithmetic optimization algorithm," *Computer Methods in Applied Mechanics and Engineering*, vol.376, article no.113609, 2021.

[15] A. M. Furtado, F. Bradaschia, M. C. Cavalcanti, and L. R. Limongi, "A reduced voltage range global maximum power point tracking algorithm for photovoltaic systems under partial shading conditions," *IEEE Transactions on Industrial Electronics*, vol.65, no.4, pp.3252–3262, 2017.

[16] R. K. Pachauri, O. P. Mahela, A. Sharma, J. Bai, Y. K. Chauhan, B. Khan, *et al.*, " Impact of partial shading on various PV array configurations and different modeling approaches: A comprehensive review," *IEEE Access* , vol.8, pp.181375–181403, 2020.

[17] L. Samani and R. Mirzaei, " Maximum power point tracking for photovoltaic systems under partial shading conditions via modified model predictive control," *Electrical Engineering*, vol.103, pp.1923–1947, 2021.

Saeid Bairami was born in Ardabil, Iran, in 1981. He received the M.S. degrees in mechatronics from Semnan University, Semnan, Iran, in 2007. Since 2007, he has been with the Faculty of Electrical Engineering at Islamic Azad University, Ardabil Branch, Ardabil, Iran, where he is a Professor of Electrical Engineering. His research interests include renewable energy, mechatronics, photovoltaic, power system planning and power electronics applications.
(Email: saeid.bairami@gmail.com)

Mahdi Salimi (corresponding author) graduated in electrical engineering from Islamic Azad University (IAU) (Science and Research Branch), Tehran, Iran, in 2012. He worked as an Assistant Professor from 2012 until 2019 at the IAU University, Ardabil Branch, Iran, in the Electrical and Electronics Department. In 2019 he joined the University of Nottingham, Power Electronics, Machine, and Control (PEMC) Group as a Researcher for three years. Since April 2022, he has worked at Greenwich University as a Lecturer of power electronics. He has published 31 papers in peer-reviewed journals with 24 papers published in international conferences. His research areas include design, closed-loop control, simulation, and practical implementation of the power electronics systems for more or full electric aircraft and vehicles, grid-connected renewable energy systems, and active power filters.
(Email: m.salimi@greenwich.ac.uk)

Davar Mirabbasi was born in Ardabil, Iran, in 1982. He received the Ph.D. degree in electrical engineering from Shahid Chamran University of Ahwaz, Ahwaz, Iran, in 2014. Since 2006, he has been with the Faculty of Electrical Engineering at Islamic Azad University, Ardabil Branch, Ardabil, Iran, where he is a Professor of Electrical Engineering. His research interests include smart grids, power system planning, and power electronics applications.
(Email: dmirabbasi@iauardabil.ac.ir)